

# Numerical Study of Nitrogen Oxides (NO<sub>x</sub>) Formation in Homogenous System of Methane, Methanol and Methyl Formate at High Pressures

J. M. Ngugi, P. N. Kioni, and J. K. Tanui

**Abstract**—The main aim of this study is to determine the effect of equivalence ratio and pressure on the formation of nitrogen oxides (NO<sub>x</sub>) in homogenous ignition of methane/air, methanol/air and methyl formate/air. A constant volume reactor of 200 cm<sup>3</sup>, at initial temperature of 1300 K and at pressure, P, ranging between 1-50 atmospheres has been considered. The equivalence ratios of the test mixtures have been varied from 0.7 to 1.3. This represents the lean-to-rich region which is most relevant to the conditions in an internal combustion engine. CH<sub>4</sub>, CH<sub>3</sub>OH and CH<sub>3</sub>OCHO flames have been modelled with different detailed reactions mechanisms, which have been modified and extended to incorporate high pressure oxidation reactions. Flame structures, minor species and NO<sub>x</sub> time histories have been plotted for the three fuels under different conditions. The results obtained show that the formation of NO<sub>x</sub> vary with pressure and equivalence ratios. NO mole fraction profiles and other radicals; N<sub>2</sub>, N, O, OH, CH, HCN, and N<sub>2</sub>O that are dominant in formation of NO have been compared. It is established that in homogenous system, NO formation is high in CH<sub>4</sub> at lean and stoichiometric conditions while CH<sub>3</sub>OCHO has high NO at rich conditions for all pressures. At fuel lean and stoichiometric conditions, as pressure increase from 1 to 50 atm peak NO formed in all the three fuels increases. At fuel rich condition, as pressure increase from 1 to 50 atm peak NO formed in all the three fuels decrease. High concentration of N<sub>2</sub>, O, OH and high temperatures observed in all flames indicate that Zel'dovich mechanism is the main NO formation route in a homogenous reactor.

**Index Terms**—Methane, methanol, methyl formate, nitric oxide, homogenous system.

## I. INTRODUCTION

The reduction in fossil fuel reserves and the need to reduce environmental pollution has promoted the development of renewable and alternative fuels. Biodiesel fuels (methyl esters fuels) has been investigated as alternative transportation fuels because of their ability to reduce the emissions of CO, particulate matter and unburnt hydrocarbons as noted by Basha and Gopal [1]. Liu *et al.* [2], showed that biodiesel fuels give higher thermal efficiencies than diesel at various engine speeds. Biodiesel fuels typically contain about 10-15 % or greater oxygen content by mass. The presence of oxygen atom in the structure of the biodiesel fuels makes the fuel to burn more efficiently with reduced emissions of soot, unburnt hydrocarbons and carbon

monoxide as noted by Ekarong [3]. However, as noted by Michael *et al.* [4] and Magin *et al.* [5], combustion of biodiesel fuels produces more nitrogen oxides (NO<sub>x</sub>) compared to fossil fuels. NO<sub>x</sub> are pollutants whose reduction is a major issue in the design of combustion devices. The purpose of the study reported herein is to determine the NO<sub>x</sub> formation mechanism in in homogenous premixed combustion of esters.

Biodiesel is produced from vegetable oils through a transesterification process. The alcohol commonly used in this process is methanol. For this reason, most common bio-diesel fuels are methyl-esters. Typical biodiesel consists of mixtures of saturated and unsaturated long-chain fatty acid methyl-esters with 1520 or more carbon atoms in their alkyl chain. The chemical kinetics involved in combustion of these large ester species are complex due to the formation of many intermediate species. This makes the computations involved during kinetic modeling of real fuels more difficult to analyze. Hence, fuels of simpler chemical structure, referred to as surrogate fuels, are used to approximate or represent processes involved in the combustion of these real fuels, as reported by Dooley *et al.* [6], [7] and Francisco [8]. In this regard, esters with a low number of carbon atoms are adopted as surrogate fuels. The simpler structure is amenable to more detailed chemical kinetics study.

To this end, methyl formate (CH<sub>3</sub>OCHO), the smallest methyl ester molecule, is well suited for the studies of esters and hence biodiesel. In this regard, also, methane (CH<sub>4</sub>) is a suitable representative of fossil fuels, viz., hydrocarbon fuels for the purpose of determining the influence of oxygenation on NO<sub>x</sub> formation. Methanol (CH<sub>3</sub>OH) chemical species appears quite prominently in the CH<sub>3</sub>OCHO detailed chemical kinetics. Furthermore, it is used in transesterification and has one carbon chemical structure comparable to that of methyl formate and methane. There is a lot of data, experimental, theoretical and numerical, on oxidation of CH<sub>4</sub> and CH<sub>3</sub>OH and this provides a good basis for further studies incorporating NO<sub>x</sub> formation mechanism, and for validating the solution obtained in new studies.

CH<sub>3</sub>OCHO has been a subject of various experimental and kinetic modeling studies that have mainly focused on decomposition pathway, development of kinetic modeling parameters and species formation. Dooley *et al.* [6] reported a detailed oxidation mechanism of methyl formate. This mechanism is based on experimental data obtained from flow reactor studies, shock tube ignition delays and laminar burning velocity. Dooley *et al.* [7] have also reported oxidation of methyl formate in a series of burner stabilized laminar flames at low-pressures of 0.03-0.04 bar and fuel-air

Manuscript received February 20, 2017; revised June 12, 2017. This work was supported by Dedan Kimathi University of Technology.

J. M. Ngugi, P. N. Kioni and J.K. Tanui are with Department of Mechanical Engineering, Dedan Kimathi University of Technology P.O. Box 657-10100, Nyeri, Kenya (e-mail: ndirangukioni@dkut.ac.ke).

equivalence ratios from 1.0 to 1.8. The kinetic mechanism did not incorporate NO<sub>x</sub> formation.

#### A. Combustion Kinetics at High Pressures

Most combustion chemistry studies have focused on normal pressures, viz., 1 atmosphere, much lower than the typical pressure range of 20-50 atm experienced in internal combustion engines. Thus, better insight of the NO<sub>x</sub> formation may be obtained by simulating combustion at these higher pressures. This requires the knowledge of high pressure rate constants and/or the dependence of rate constants on pressure.

According to Dooley *et al.* [6], the computation of the high pressure rate constant, the dependence of rate constant on pressure and the determination of collision energy transfer parameter are the major uncertainties in kinetic modeling of methyl formate flames. Either Quantum-Rice-Ramsperger Kassel (QRRK) or Rice-Ramsperger-Kassel-Markus (RRKM) theory (Dooley *et al.* [6]) may be applied to estimate the rate constant at higher pressure combustion. Metcalfe *et al.* [9] computed pressure-dependent rate constants for methyl formate decomposition using Rice-Ramsperger-Kassel-Markus (RRKM) theory. Dooley *et al.* [6] evaluated the performance of QRRK and RRKM high pressure rate constants for the major methyl formate decomposition channel, CH<sub>3</sub>OCHO $\rightleftharpoons$ CH<sub>3</sub>OH+CO against methanol measurement and observed that the QRRK rate parameters give peak methanol values that are very close to the peak experimental values.

Oxidation of methane at high pressures has been investigated by various researchers Hunter *et al.* [10], Petersen *et al.* [11], Sibendu *et al.* [12] and Curran [13]. Thomsen *et al.* [14], modeled NO formation in premixed, high-pressure methane flames and showed that GRI-Mech 2.11 mechanism is not suitable for the quantitative prediction of NO concentrations in rich, premixed flames. Sibendu *et al.* [12] used three different mechanisms namely GRI-Mech 2.11, GRI-Mech 3.0 and the San Diego mechanism to investigate the effect of pressure on flame structure. At normal pressures, there was agreement for all the mechanisms between the simulations and the experiments. However, beyond a critical pressure of 11 bar, the structure and temperature profiles of the premixed flame changed significantly [12]. Rozenchan *et al.* [15], reported numerical and experimental investigation of laminar burning velocities and chemical effects of methane/oxidizer flames up to 60 atm. Simulations using GRI-Mech 3.0 in this case showed satisfactory agreement with experimental data up to 20 atm and moderate deviation for pressures above 40 atm. Petersen *et al.* [11] investigated methane/oxygen ignition at elevated pressures (40-260 atm) and intermediate temperatures (1040-1500 K) and various equivalence ratios. Reactions involving HO<sub>2</sub>, CH<sub>3</sub>O<sub>2</sub> and H<sub>2</sub>O<sub>2</sub> were identified as major reactions needed to model methane oxidation at conditions of high pressure and intermediate temperatures.

Methanol is an oxygenated fuel which is also one of the alcohol currently used as alternative fuels or as additives to transportation fuels to improve performance. Held and Dryer [16] developed a comprehensive detailed mechanism for methanol oxidation. This mechanism has been validated against multiple experimental data sets: flow reactor, static

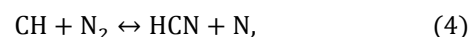
reactor, shock tube, premixed flame experiments and counter flow diffusion flames. The mechanism covers conditions of temperature from 633 to 2050 K, pressure from 0.26 to 20 atm and equivalence ratios from 0.05 to 2.6. In Sheng *et al.* [17], the pressure and temperature dependent rate constants were obtained by utilizing QRRK theory over a pressure range of 0.01-100 atm and temperature range of 250-2500 K.

#### B. Chemical Kinetics of NO<sub>x</sub> Formation

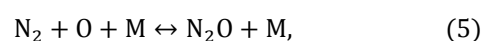
Nitrogen oxides NO<sub>x</sub> are composed of nitric oxide, NO and nitrogen dioxide NO<sub>2</sub>. The four main routes of NO formation in combustion processes are Zel'dovich mechanism (thermo NO), N<sub>2</sub>O route, prompt-NO and Fuel Bound Nitrogen (FBN). Thermo NO is formed in high temperature flame regions through extended Zel'dovich mechanism which is shown below.



Prompt-NO is formed at low temperature flame front regions due to the presence of CH radicals. The CH radical reacts with molecular nitrogen according to Eq. (4). The nitrogen generated from this mechanism proceeds to form NO through Eq. (2) and Eq. (3).



NO production through N<sub>2</sub>O route occurs through the free body recombination reactions, Eq. (5), under the conditions of high pressures.



where *M* is an energy carrier. The N<sub>2</sub>O formed in Eq. (5) reacts with O to form NO through Eq. (6).



Combustion of fuels that contain nitrogen results in formation of NO<sub>x</sub>. Most fuels used in internal combustion engines contains contain very little or no Fuel Bound Nitrogen, as noted by DeCorso and Clark [18], and hence, Fuel NO<sub>x</sub> is neglected in this work.

In Kioni *et al.* [19], kinetic modeling study of NO formation in methyl formate flames in freely propagating flames, homogenous system and counter flow diffusion flames at low pressures, 1 bar, and equivalence ratio of 1 showed low NO formation in this fuel when compared to the case of methane/air and methanol/air in all the three flow configurations. This is not in agreement with prior experimental investigations by Rao [20] and Gerhard *et al.* [21] that have reported high NO formation in biodiesel. In this work, the effect of pressure  $\phi$  on the formation of NO in homogenous system of CH<sub>3</sub>OCHO is investigated. The results obtained are compared with those of methane and methanol under the same conditions. This is important

because combustion in diesel engines occurs at high pressures, high temperatures and at various fuel-air equivalence ratios.

This paper is presented in four sections. Following this introduction is the modelling which covers the mathematical problem, the reaction equations and kinetics; and the solution method. Next is the results and discussion section which is followed by conclusions.

## II. NUMERICAL MODELING

The experimental conditions behind the reflected shock wave are modeled as constant volume and homogenous adiabatic mixture with constant internal energy. Thus, ignition in a shock tube is simulated as zero-space dimension homogenous system as shown in Fig. 1. The time which we denote by  $t$  is the only independent variable in a transient homogenous system.

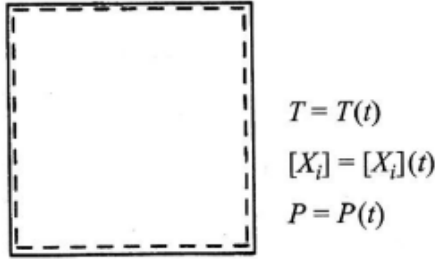


Fig. 1. Perfectly mixed homogenous reactor.

The simulation of transient zero-spatial dimensional system requires solution of the partial differential equations for conservation of energy, chemical species and the equation of state. The full set of these equations is presented below. However, details on the derivations are omitted as they are available in a number of literature sources; for example, Turns [22] and Williams [23].

- Species conservation equation

$$\rho \frac{dY_k}{dt} = w_k \quad (7)$$

- Energy conservation equation

$$c_v \rho \frac{dT}{dt} + \frac{P}{V} \frac{dV}{dt} = - \sum_{i=1}^N \mu_i w_i + \frac{Q}{V} \quad (8)$$

where  $c_v$  is specific heat at constant volume given by  $c_v = \sum_{i=1}^N Y_i c_{v,i}$ ,

- Equation of state

$$P = \rho RT \sum_{i=1}^N \left( \frac{Y_i}{W_i} \right). \quad (9)$$

In Eqs. (7)-(9),  $V$  is the instantaneous reactor volume, and  $Q$  is the rate of heat transfer across the walls of the reactor. The volume  $V$  of the reactor in this case is given. Therefore, pressure  $P$  is a time dependent quantity to be determined as part of the solution. where  $k = c_p/c_v$ . Equations (7), (8) and (10) are solved numerically for given initial values of  $T$ ,  $P$ ,  $Y_i$ , for  $i=1, \dots, N$ .

### A. Initial and Boundary Conditions

In this work, the numerical simulations for methane/air, methanol/air and methyl formate/air flames are for the following conditions: A constant volume of 200 cm<sup>3</sup>, at initial temperature of 1300 K and at pressure,  $P$ , ranging between 1-50 atmospheres. The equivalence ratios of the test mixtures have been varied from 0.7 to 1.3. This represents the lean-to-rich region which is most relevant to the conditions in an internal combustion engine.

TABLE I: ADDITIONAL REACTIONS FOR METHANE SYSTEM AT HIGH-PRESSURES (HUNTER *ET AL.* 1994, PETERSEN *ET AL.* 1999).

Reaction	A	n	Activation Energy cal/mol
CH <sub>3</sub> O <sub>2</sub> +H ⇌ CH <sub>3</sub> O+OH	9.6E+013	0.00	0.00
CH <sub>3</sub> O <sub>2</sub> +O ⇌ CH <sub>3</sub> O+O <sub>2</sub>	3.6E+013	0.00	0.00
CH <sub>3</sub> O <sub>2</sub> +OH ⇌ CH <sub>3</sub> OH+O <sub>2</sub>	6.0E+013	0.00	0.00
CH <sub>3</sub> O <sub>2</sub> +HO <sub>2</sub> ⇌ CH <sub>3</sub> O <sub>2</sub> H+O <sub>2</sub>	4.6E+010	0.00	-2581.20
CH <sub>3</sub> O <sub>2</sub> +HCO ⇌ CH <sub>3</sub> O+H+CO <sub>2</sub>	3.0E+013	0.00	0.00
CH <sub>3</sub> O <sub>2</sub> +CH <sub>3</sub> ⇌ CH <sub>3</sub> O+CH <sub>3</sub> O	2.0E+013	0.00	0.00
CH <sub>3</sub> O <sub>2</sub> +H <sub>2</sub> O <sub>2</sub> ⇌ CH <sub>3</sub> O <sub>2</sub> H+HO <sub>2</sub>	2.4E+012	0.00	9942.40
CH <sub>3</sub> O <sub>2</sub> +CH <sub>2</sub> O ⇌ CH <sub>3</sub> O <sub>2</sub> H+HCO	2.0E+012	0.00	11663.20
CH <sub>3</sub> O <sub>2</sub> +CH <sub>3</sub> O <sub>2</sub> ⇌ CH <sub>3</sub> O+CH <sub>3</sub> O+O <sub>2</sub>	7.8E+010	0.00	0.00
CH <sub>3</sub> O <sub>2</sub> +CH <sub>3</sub> O <sub>2</sub> ⇌ CH <sub>3</sub> OH+CH <sub>2</sub> O+O <sub>2</sub>	1.3E+011	0.00	0.00
H <sub>2</sub> O <sub>2</sub> +M ⇌ OH+OH+M	1.0E+017	0.00	45410.00
H+H <sub>2</sub> O <sub>2</sub> ⇌ HO <sub>2</sub> +H <sub>2</sub>	1.7E+012	0.00	3752.30
H+H <sub>2</sub> O <sub>2</sub> ⇌ OH+H <sub>2</sub> O	1.0E+013	0.00	3585.00
OH+H <sub>2</sub> O <sub>2</sub> ⇌ HO <sub>2</sub> +H <sub>2</sub> O	7.0E+012	0.00	1434.00
O+H <sub>2</sub> O <sub>2</sub> ⇌ OH+HO <sub>2</sub>	2.8E+013	0.00	6405.00
O+HO <sub>2</sub> ⇌ OH+O <sub>2</sub>	2.0E+013	0.00	0.00
H+HO <sub>2</sub> ⇌ O+H <sub>2</sub> O	5.0E+012	0.00	1410.10
H+HO <sub>2</sub> ⇌ O <sub>2</sub> +H <sub>2</sub>	2.5E+013	0.00	693.10
H+HO <sub>2</sub> ⇌ OH+OH	1.5E+014	0.00	1003.80
OH+HO <sub>2</sub> ⇌ O <sub>2</sub> +H <sub>2</sub> O	6.0E+013	0.00	0.00
HO <sub>2</sub> +HO <sub>2</sub> ⇌ O <sub>2</sub> +H <sub>2</sub> O <sub>2</sub>	4.2E+014	0.00	11973.90

TABLE II: HIGH-PRESSURE LIMIT RATE COEFFICIENTS FOR THE CH<sub>3</sub>OH AND CH<sub>3</sub>OCHO (SHENG *ET AL.* 2002)

Reaction	A	n	Activation Energy (cal/mol)
CH <sub>3</sub> +OH=CH <sub>3</sub> OH	3.3133E06	2.07650	-1755.10
CH <sub>3</sub> OH=CH <sub>3</sub> +OH	3.2591E10	2.05451	90347.00
CH <sub>3</sub> OH=CH <sub>2</sub> OH+H	1.6369E07	2.54513	91951.00
CH <sub>3</sub> OH=CH <sub>3</sub> O+H	1.1908E07	2.38792	99614.00
CH <sub>3</sub> OH=CH <sub>2</sub> O+H <sub>2</sub>	1.1004E09	1.28149	90233.00
CH <sub>3</sub> OH=HCOH+H <sub>2</sub>	2.0299E10	1.22342	86411.00
CH <sub>3</sub> OH=CH <sub>2</sub> +H <sub>2</sub> O	2.8735E11	1.60030	92538.00

### B. Numerical Solution Method

The numerical solution method for the governing equations, and determination of transport and thermodynamics data are provided by Rogg [23]. The numerical solution for the governing equations is implemented in RUN1D1 code in COSILAB software package [24].

### C. Chemical Kinetics

The reaction mechanism for methane is the GRI-3.0 reaction mechanism [25] which is then modified and extended using additional reactions given in Curran [14] and Petersen *et al.* [12] so as to cover the methane oxidation at high pressures. The latter additional reaction equations are presented in Table I. Methanol flames are computed using a comprehensive mechanism by Held and Dryer [17] combined with Leeds NO<sub>x</sub> oxidation mechanism. The mechanism has also been modified and extended with high pressure rate coefficients reported by Sheng *et al.* [18] and herein given in Table II. Finally, methyl formate flames reaction mechanism is that reported by the Dooley *et al.* [6] combined with the Leeds NO<sub>x</sub> mechanism. It is further modified with QRRK high pressure rate parameters for the major decomposition channel, CH<sub>3</sub>OCHO=CH<sub>3</sub>OH+CO as proposed by Dooley *et al.* [7]. This mechanism incorporates high pressure rate coefficients for methanol mechanism given in Table II.

## III. RESULTS AND DISCUSSIONS

The temperature profiles for the three fuel/air mixtures at 1

and 50 atm for equivalence ratios 0.7 and 1.3 are shown in Fig. 2 and Fig. 3. The figures show that temperature increases with increase in pressure at the three equivalence ratios; for instance, at  $\phi = 1.3$  the peak temperatures for 1 atm case in methane, methanol and methyl formate are 2890 K, 2870 K and 2860 K. When, the pressure is increased to 50 atm, the corresponding peak pressures for methane, methanol and methyl formate are 3160 K, 3150 K and 3160 K. This represents a percentage increase of 9.34 %, 9.75 % and 10.48 % in methane, methanol and methyl formate respectively. The increase in temperature with pressure is attributed to the fact that temperature and pressure are proportional as specified in the equation of state.

Comparison of temperature profiles and other species concentration profiles for methane, methanol and methyl formate for the homogenous case shows that methane profiles lag behind those of methanol and methyl formate. This is because methane has longer ignition delay, hence, methane/air reaction takes a longer time to start. Figures 4, 5 and 6 are the species concentration profiles for NO at pressures of 1 and 50 atmospheres for equivalence ratios of 0.7, 1.0 and 1.3 respectively. The figures show that NO formation in the three fuels vary with pressure and equivalence ratio. At  $\phi = 0.7$ , increase in pressure from 1 to 50 atm increases peak NO formation by 25.3 %, 30 % and 30.3 % in CH<sub>4</sub>, CH<sub>3</sub>OH and CH<sub>3</sub>OCHO respectively. While at  $\phi = 1.0$ , the corresponding percentage increase in NO formation are 8.1 %, 13.77 % and 15 %. At  $\phi = 1.3$ , increase in pressure from 1 to 50 atm results to a percentage decrease of 40.7 %, 27.47 % and 19.5 % respectively in CH<sub>4</sub>, CH<sub>3</sub>OH and CH<sub>3</sub>OCHO.

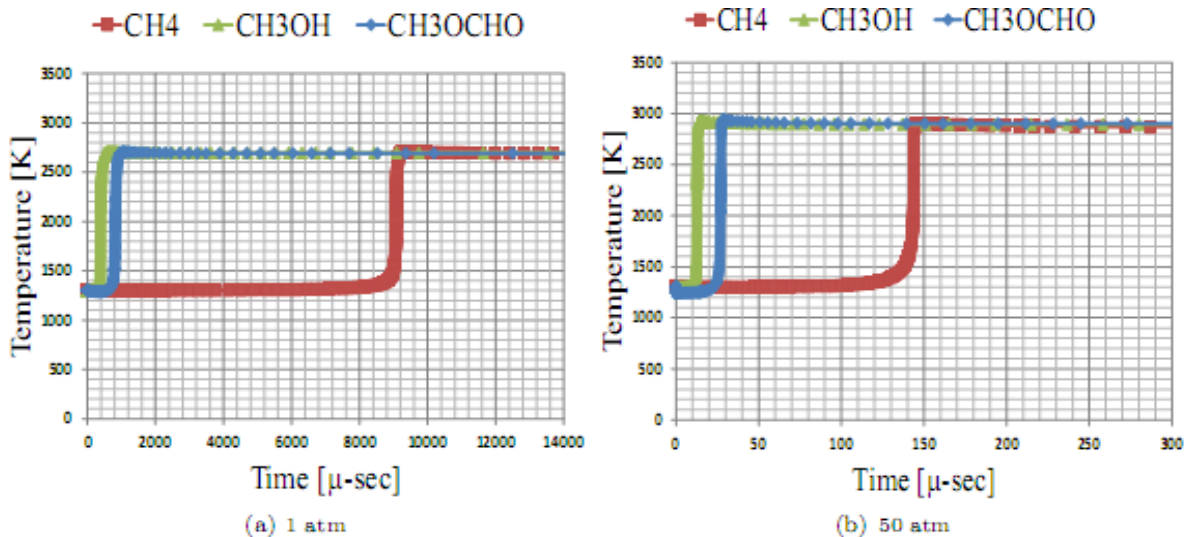


Fig. 2. CH<sub>4</sub>/air, CH<sub>3</sub>OH/air and CH<sub>3</sub>OCHO/air shock tube temperature profiles ( $\phi = 0.7$ ).

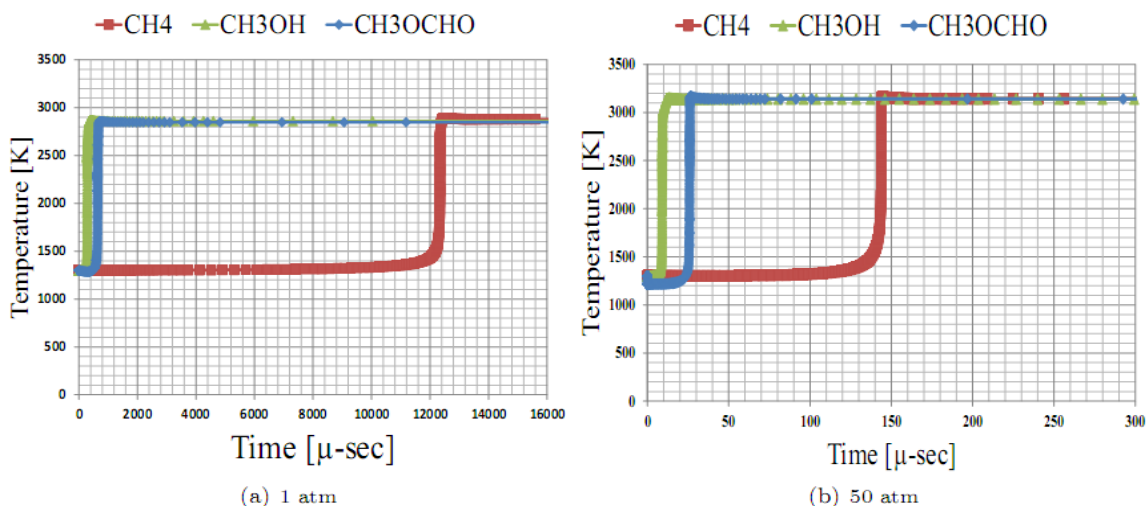


Fig. 3. CH<sub>4</sub>/air, CH<sub>3</sub>OH/air and CH<sub>3</sub>OCHO/air shock tube temperature profiles ( $\phi = 1.3$ ).

Fig. 4-Fig. 6 also show that more NO formation is observed at  $\phi = 0.7$  for all the three fuels when compared to NO formation at  $\phi = 1.0$  and  $\phi = 1.3$ . For instance, at 50 atm, CH<sub>3</sub>OCHO produces approximately 17200, 11200 and 500 ppm moles of NO at  $\phi = 0.7$ , 1.0 and 1.3 respectively. Comparison of NO formation in CH<sub>4</sub>, CH<sub>3</sub>OH and CH<sub>3</sub>OCHO show that CH<sub>4</sub> produces more NO at  $\phi = 0.7$  and  $\phi = 1.0$  at 1 atm and 50 atm compared NO formation CH<sub>3</sub>O

and CH<sub>3</sub>OCHO. On the other hand, CH<sub>3</sub>OCHO produces more NO at  $\phi = 1.3$  as shown in Fig. 6. For instance, at  $\phi = 1.3$  and 50 atm, CH<sub>4</sub>, CH<sub>3</sub>OH and CH<sub>3</sub>OCHO produces 3200, 3500 and 4900 ppm moles of NO. The difference in formation of NO in CH<sub>4</sub>, CH<sub>3</sub>OH and CH<sub>3</sub>OCHO at the various equivalence ratios and pressures is attributed to the differences in evolution of the various species that affect formation of NO.

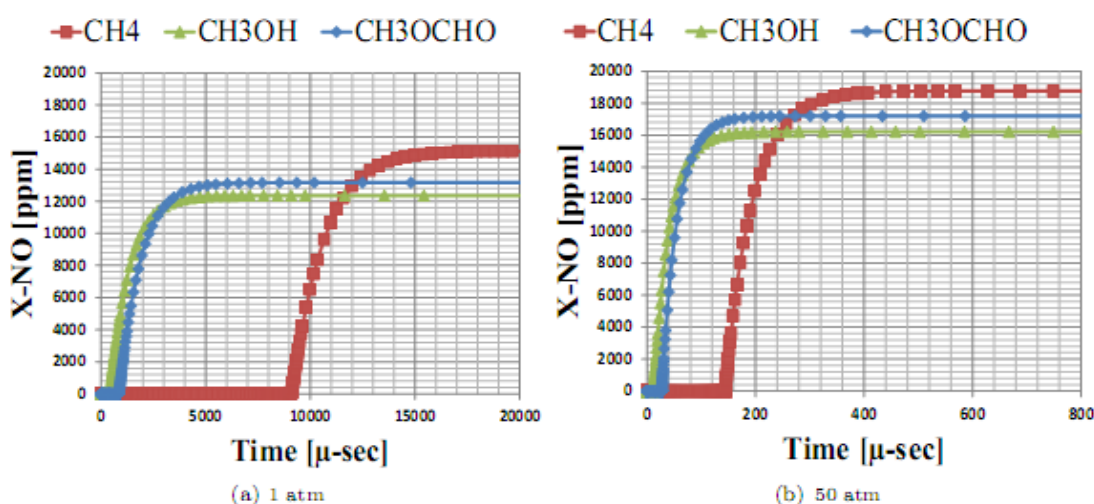


Fig. 4. NO concentration profiles for CH<sub>4</sub>/air, CH<sub>3</sub>OH/air and CH<sub>3</sub>OCHO/air mixtures ( $\phi = 0.7$ ).

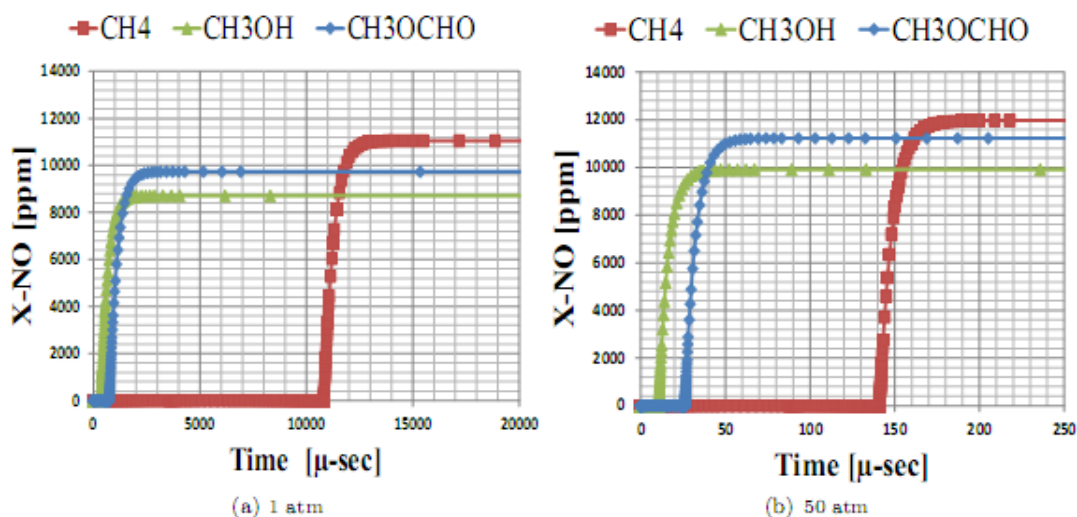


Fig. 5. NO concentration profiles for CH<sub>4</sub>/air, CH<sub>3</sub>OH/air and CH<sub>3</sub>OCHO/air mixtures ( $\phi = 0.7$ ).

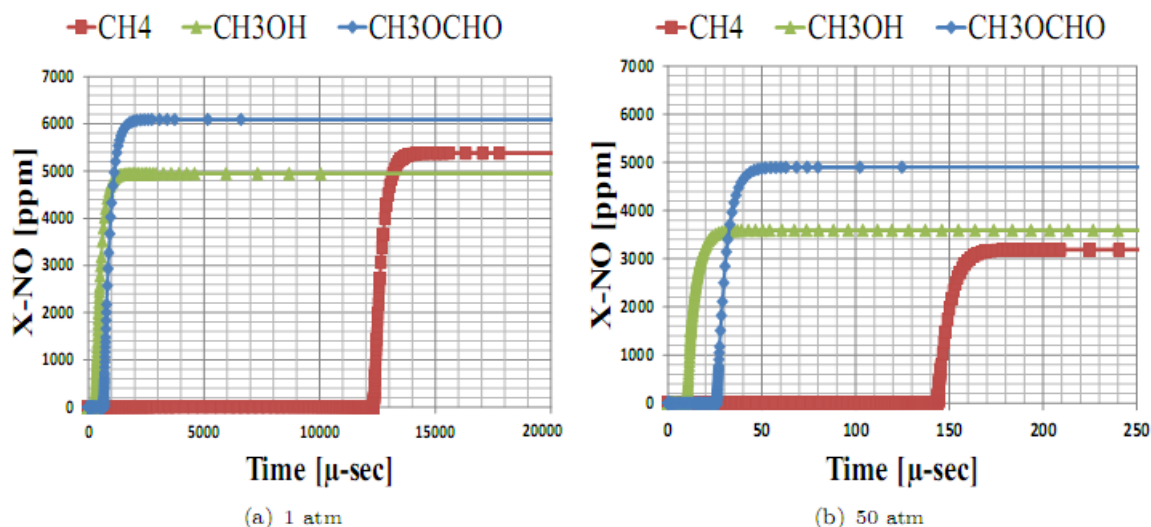


Fig. 6. NO concentration profiles for CH<sub>4</sub>/air, CH<sub>3</sub>OH/air and CH<sub>3</sub>OCHO/air mixtures ( $\phi = 1.3$ ).

Fig. 7 presents the variation of N<sub>2</sub> with equivalence ratio for the three test fuels. The N<sub>2</sub> mole fraction profiles at 1 atm are high in CH<sub>4</sub> when compared to CH<sub>3</sub>OH and CH<sub>3</sub>OCHO. This is expected since the chemically bonded oxygen molecules in CH<sub>3</sub>OH and CH<sub>3</sub>OCHO lowers the amount of air required during their combustion. Methane being an un-oxygenated fuel requires more air and hence nitrogen

molecules. Fig. 7 also shows a decrease of N<sub>2</sub> with equivalence ratio which is attributed to the reduction in oxidizer (air) as fuel-air equivalence ratio increases. N<sub>2</sub> is an important species in the formation of NO, N<sub>2</sub>O and other N-related species; this explains the reduction in N<sub>2</sub> with time in all the three fuels.

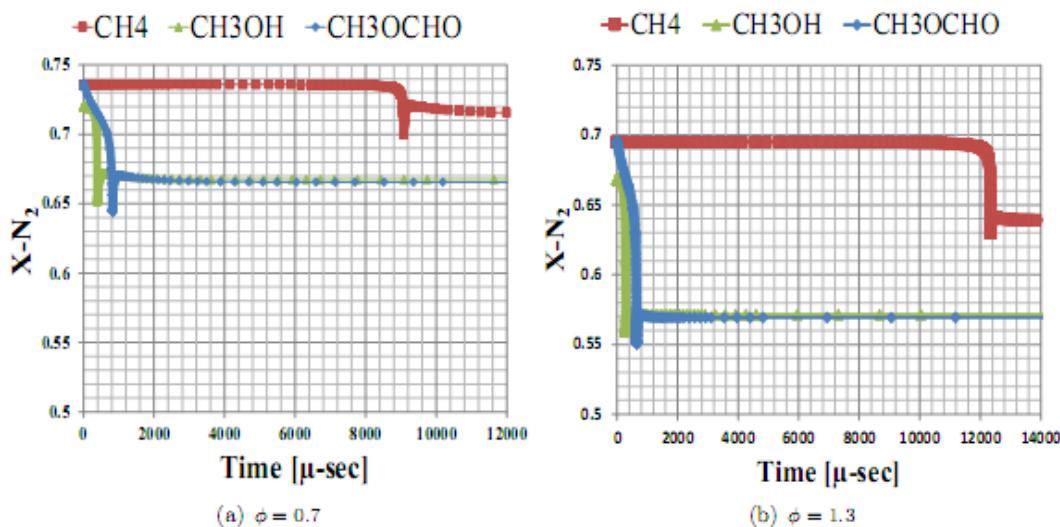


Fig. 7. N<sub>2</sub> concentration profiles for CH<sub>4</sub>/air, CH<sub>3</sub>OH/air and CH<sub>3</sub>OCHO/air mixtures at 1 atm.

Comparison of N radical formation at equivalence ratios of 0.7 and 1.3 shows more N radicals are formed at rich condition than at lean conditions for all the pressures considered as shown in Fig. 8 and Fig. 9. Methane has slightly less N as compared to methanol and methyl formate. Fig. 8 and Fig. 9 also show that at  $\phi=0.7$  an increase in pressure from 1 atm to 50 atm decreases in peak N formation by 20.68 %, 15.38 % and 19.5 % in methane, methanol and methyl formate respectively. This is also the case with  $\phi=1.0$  and  $\phi=1.3$ . N is an important species in the formation of NO through Zel'dovich reactions;  $N+O_2 \rightarrow NO+O$  and  $N+OH \rightarrow NO+H$ . From these reactions O and OH radicals are also important species in the formation of NO. Fig. 10 and Fig. 11, show the variation of mole fraction profiles of CH<sub>4</sub>, CH<sub>3</sub>OH and CH<sub>3</sub>OCHO with time at  $\phi = 0.7$  and  $\phi = 1.3$ . Fig.

10 and Fig. 11 show high formation of O radicals for all the fuels and cases considered. For instance, at 1 atm, over 8000 ppm of O is observed for all the equivalence ratios.

The OH radical's concentration profiles at  $\phi = 0.7$  and  $\phi = 1.3$  are shown in Fig. 12 and Fig. 13. These figures show high formation of OH-radicals in the three fuels. For instance, at  $\phi = 0.7$  over 10000 ppm of OH radicals are formed at 1 atm and 50 atm in the three fuels. Fig. 10 and Fig. 13 show that formation of O and OH radicals increases rapidly after the onset of the reaction, reaches a peak value and then decreases gradually. The reduction is attributed to consumption these radicals in supporting other reaction among them the Zel'dovich reactions  $N+O_2 \rightarrow NO+O$  and  $N+OH \rightarrow NO+H$ .

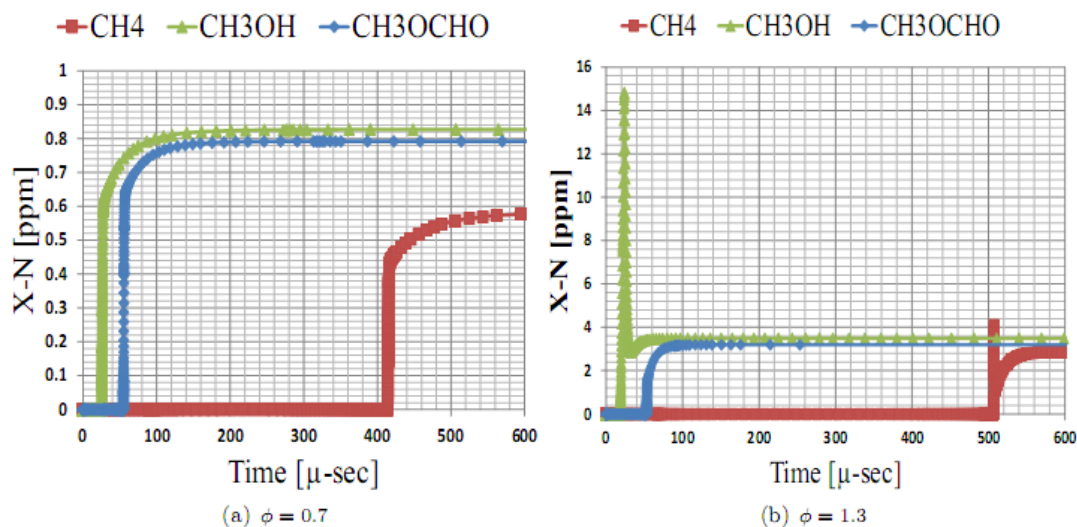


Fig. 8. N concentration profiles for CH<sub>4</sub>/air, CH<sub>3</sub>OH/air and CH<sub>3</sub>OCHO/air mixtures at 1 atm.

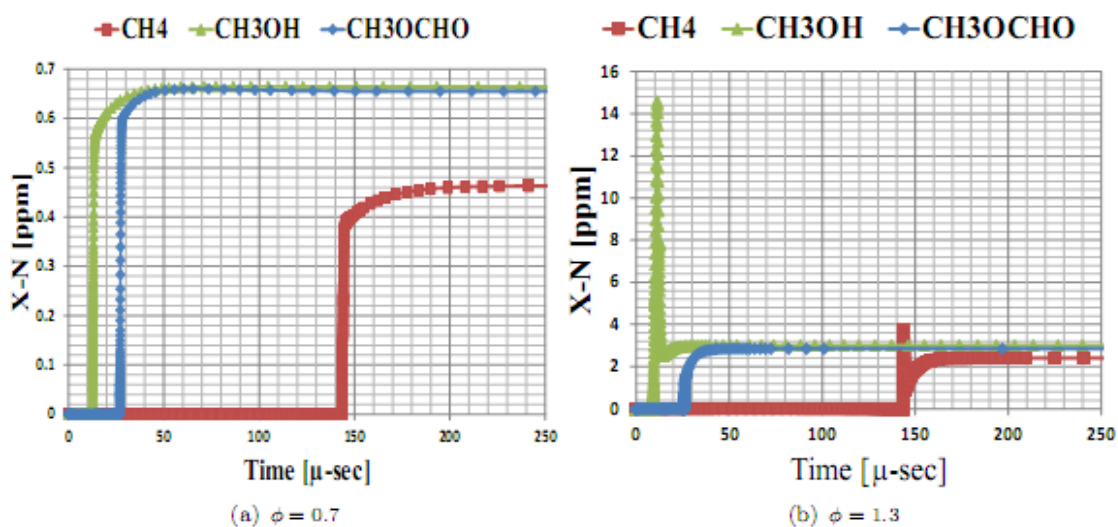


Fig. 9. N concentration profiles for CH<sub>4</sub>/air, CH<sub>3</sub>OH/air and CH<sub>3</sub>OCHO/air mixtures at 50 atm.

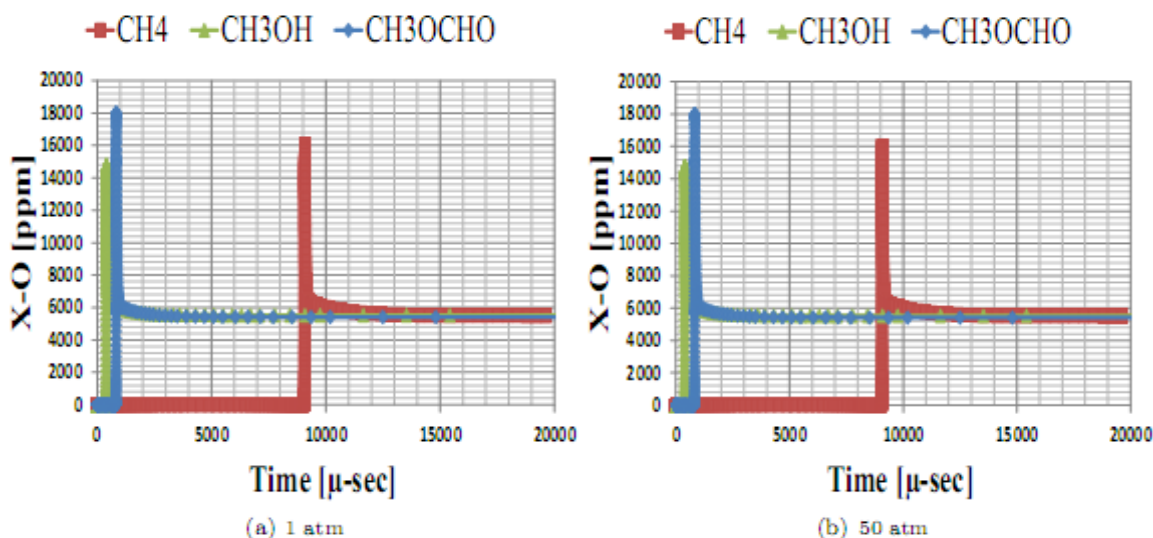


Fig. 10. O concentration profiles for CH<sub>4</sub>/air, CH<sub>3</sub>OH/air and CH<sub>3</sub>OCHO/air mixtures at ( $\phi = 0.7$ ).

The formation of NO through prompt NO route is initiated through,  $\text{CH} + \text{N}_2 \rightarrow \text{HCN} + \text{N}$ . The N radical formed reacts with O<sub>2</sub> and OH radical to form NO through,  $\text{N} + \text{O}_2 \rightarrow \text{NO} + \text{O}$  and  $\text{N} + \text{OH} \rightarrow \text{NO} + \text{H}$ . According to these figures, low levels of CH radical's production is noted in the three fuels in all the test conditions. Also, Fig. 14 and Fig. 15 show that methane

produces over 10 times more CH radicals when compared to methanol and methyl formate. This shows that the contribution of Prompt route to the total NO formed is more in methane as compared to the case of methanol and methyl formate.

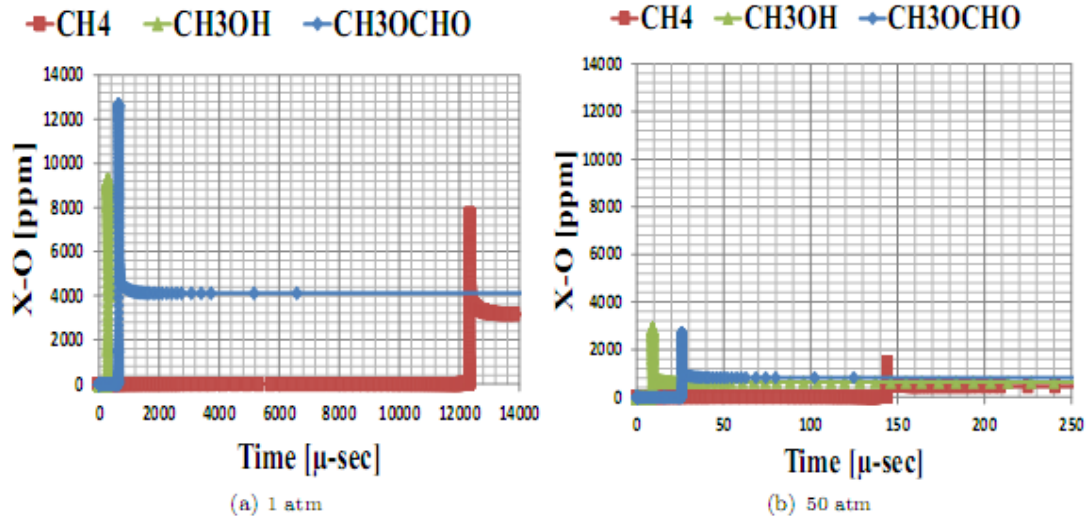


Fig. 11. O concentration profiles for CH<sub>4</sub>/air, CH<sub>3</sub>OH/air and CH<sub>3</sub>OCHO/air mixtures at ( $\phi = 1.3$ ).

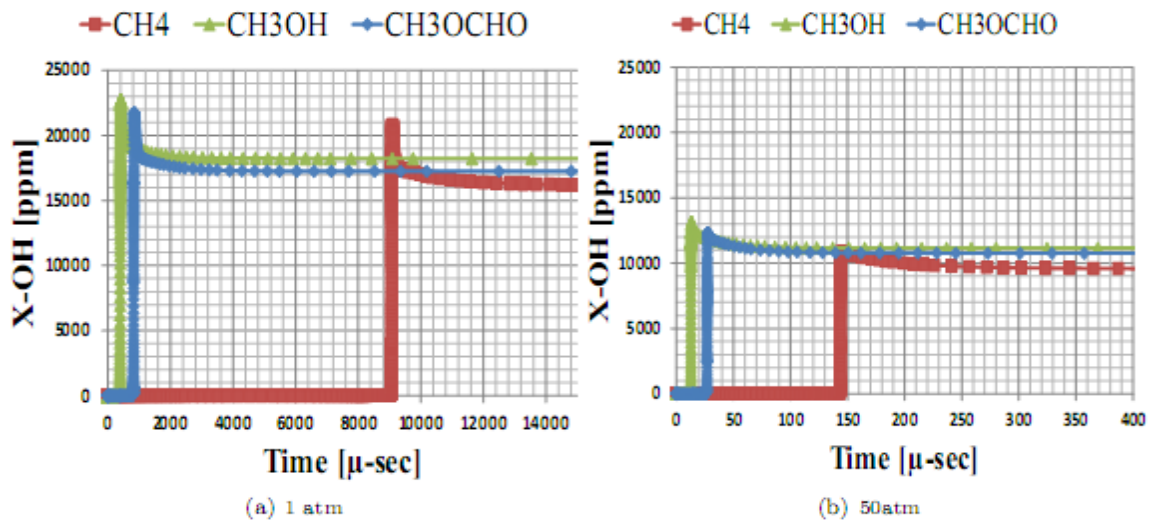


Fig. 12. OH concentration profiles for CH<sub>4</sub>/air, CH<sub>3</sub>OH/air and CH<sub>3</sub>OCHO/air mixtures at ( $\phi = 0.7$ ).

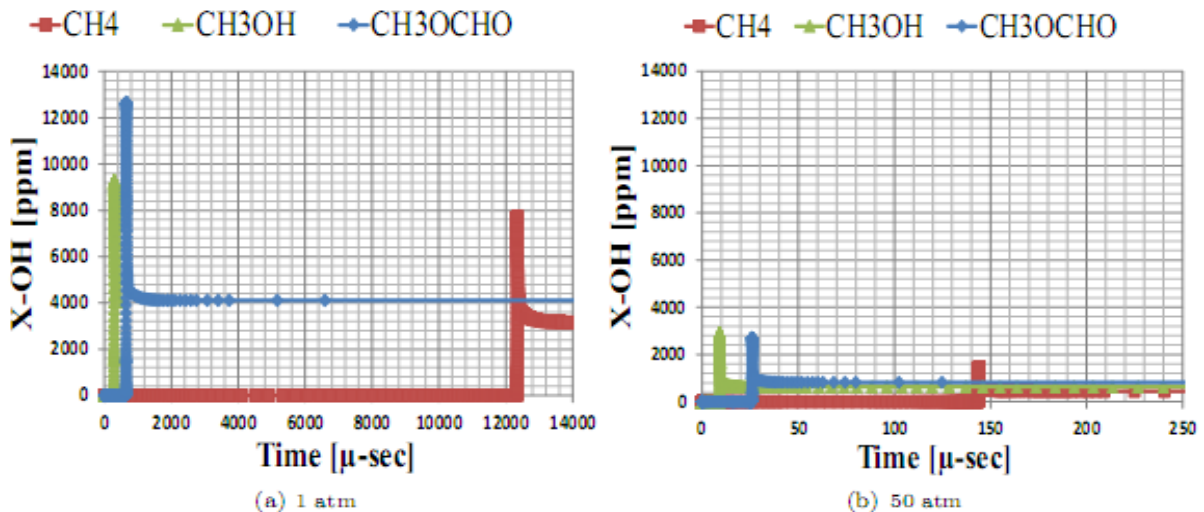


Fig. 13. OH concentration profiles for CH<sub>4</sub>/air, CH<sub>3</sub>OH/air and CH<sub>3</sub>OCHO/air mixtures at ( $\phi = 1.3$ ).

The effect of pressure in NO formation is seen through N<sub>2</sub>O route of NO production; N<sub>2</sub>+O+M→N<sub>2</sub>O+M is the rate determining step for N<sub>2</sub>O-route. This reaction occurs at conditions of high pressure. N<sub>2</sub>O is produced in relatively small amounts at low and high pressure in the three fuels as shown in Fig. 16 and Fig. 17. Equilibrium concentration of

N<sub>2</sub>O occurs at different points in time due to the variation in ignition delay time. N<sub>2</sub>O is initially high in methanol and methyl formate and decreases with time due to consumption through the following reactions; N<sub>2</sub>O+O→NO+NO, N<sub>2</sub>O+H→N<sub>2</sub>+OH, and N<sub>2</sub>O+OH→N<sub>2</sub>+HO<sub>2</sub>.



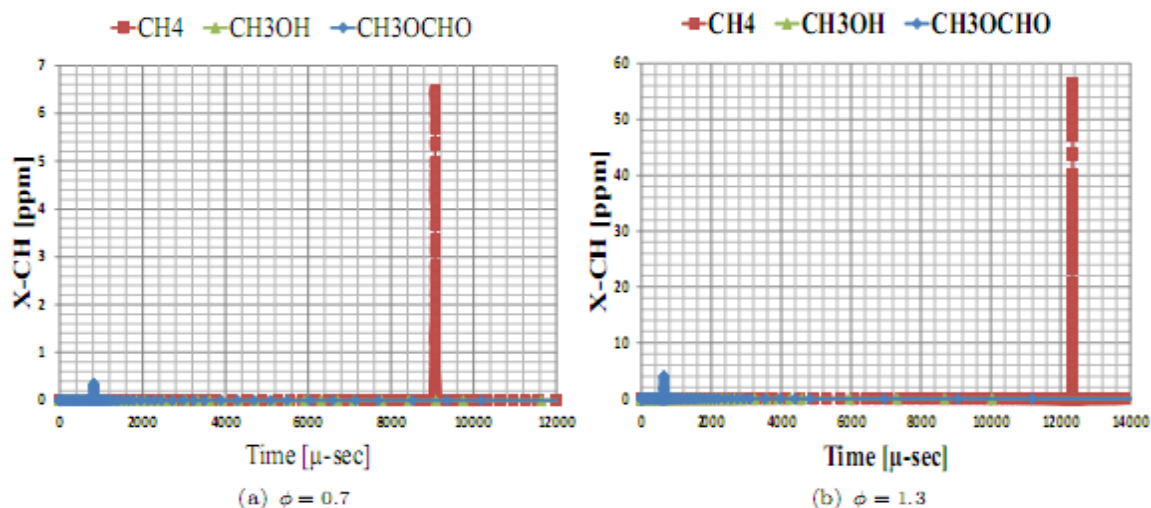


Fig. 14. CH concentration profiles for CH<sub>4</sub>/air, CH<sub>3</sub>OH/air and CH<sub>3</sub>OCHO/air mixtures at 1 atm.

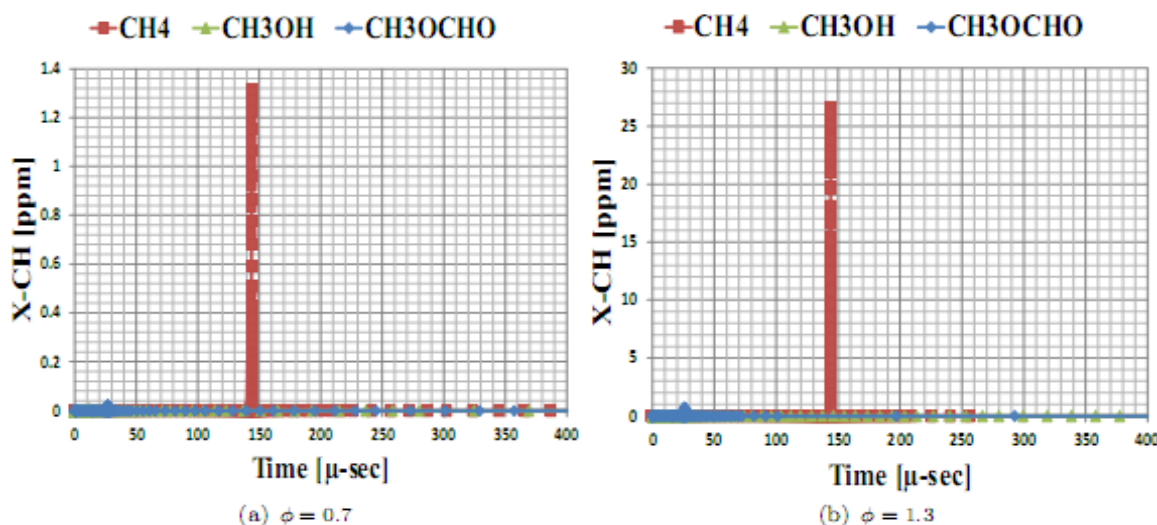


Fig. 15. CH concentration profiles for CH<sub>4</sub>/air, CH<sub>3</sub>OH/air and CH<sub>3</sub>OCHO/air mixtures at 50 atm.

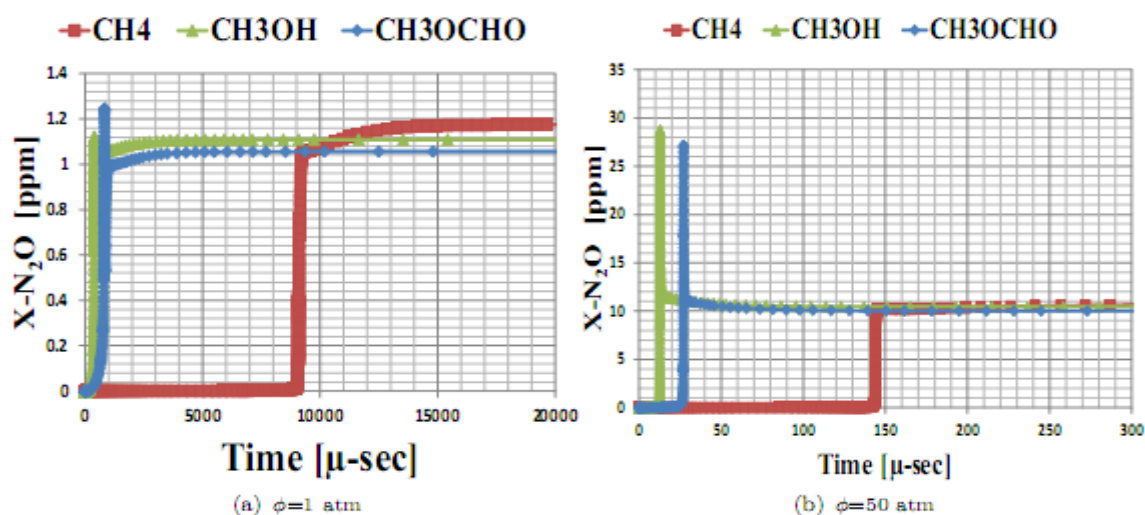


Fig. 16. N<sub>2</sub>O concentration profiles for CH<sub>4</sub>/air, CH<sub>3</sub>OH/air and CH<sub>3</sub>OCHO/air at 1 and 50 atm ( $\phi = 0.7$ ).

The comparison of N<sub>2</sub>, O, OH, N, CH and N<sub>2</sub>O mole fractions for methane, methyl formate and methanol shows that contribution of prompt NO and N<sub>2</sub>O-route to the total NO formed is negligible because of the low concentration of CH, N, and N<sub>2</sub>O mole fractions. The high concentration N<sub>2</sub>, O, and OH radicals coupled with the high temperatures of over 2700 K observed in a homogenous system implies that

Zel'dovich mechanism is the main NO formation route in a homogenous reactor. Methyl formate has the highest N, O and OH radical's concentration profiles at equivalence ratio of 1.3. Hence, the high NO formation in methyl formate at equivalence ratio of 1.3 is attributed to Zel'dovich reactions. These investigations are consistent with earlier experimental investigations by Wang *et al.* [27] and Sze *et al.* [28] that

showed NO formation in engines fueled with biodiesel decreases slightly at low loads but increases at higher loads

when engine is running at full throttle, hence more fuel.

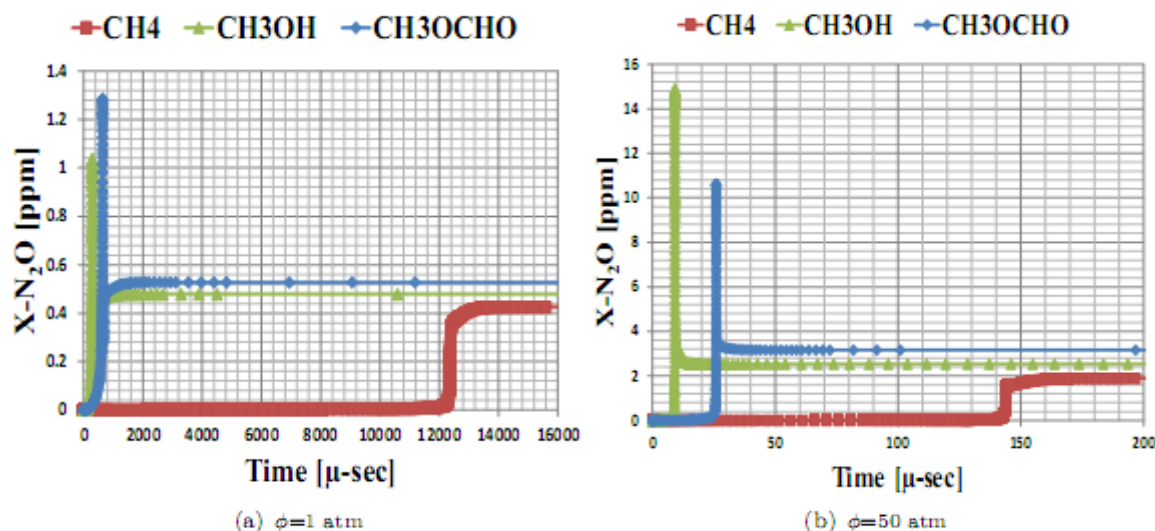


Fig. 17. N<sub>2</sub>O concentration profiles for CH<sub>4</sub>/air, CH<sub>3</sub>OH/air and CH<sub>3</sub>OCHO/air at 1 and 50 atm ( $\phi = 1.3$ ).

#### IV. CONCLUSIONS

Numerical study of NO<sub>x</sub> in homogenous ignition of CH<sub>4</sub>/air, CH<sub>3</sub>OH/air and CH<sub>3</sub>OCHO/air mixtures have been investigated at equivalent ratios of 0.7, 1.0, and 1.3 and at pressures of 1 and 50 atm. The simulations are based on modified detailed chemical kinetics to address the variation in reaction rate constants at high pressure and to incorporate NO<sub>x</sub> formation mechanisms. It is established that in homogenous system, NO formation is high in CH<sub>4</sub> at lean and stoichiometric conditions while CH<sub>3</sub>OCHO has high NO at rich conditions for all pressures. The high concentration of NO in methane at lean and stoichiometric conditions is attributed to the reaction  $N_2 + O \rightarrow NO + N$ , because of high concentration of nitrogen molecules in methane/air flame. More NO is formed in methyl formate flame at rich conditions through the reactions,  $N + O_2 \rightarrow NO + O$  and  $N + OH \rightarrow NO + H$ , because of the high concentration of N, O and OH radicals. Comparison of N<sub>2</sub>, CH and N<sub>2</sub>O mole fractions for the three flames for all the pressures and equivalence ratios considered has shown that the Zel'dovich mechanism is the main NO formation route in a homogenous reactor. The sensitivity analysis of the three fuels has shown similar sensitive reactions in oxygenated fuels, methanol and methyl formate because they have similar reaction paths.

In this work, methyl formate (CH<sub>3</sub>OCHO), the simplest methyl ester has been used to represent biodiesel. Future research work should focus on using a surrogate fuel with high molecular mass and long chain length such as methyl decanoate (C<sub>5</sub>H<sub>10</sub>O<sub>2</sub>) in order to investigate the effect of molecular structure and carbon chain length on the formation of NO in ester fuels.

#### ACKNOWLEDGMENT

The authors are grateful to Dedan Kimathi University of Technology, whose Combustion Simulation Laboratory Software package (COSILAB) was used to carry out the Flame simulations.

#### REFERENCES

- [1] S. Basha and K. Gopal, "A review on biodiesel production, combustion, emissions and performance," *International Journal of Applied Environmental Sciences*, vol. 5, pp. 23–30, 2008.
- [2] H. P. Liu, S. S. Strank, W. Mike, R. Hebner and J. Osara, "Combustion and emission modelling and testing of neat biodiesel fuel," in *Proc. the ASME 2010 4<sup>th</sup> International Conference on Energy Sustainability*, 2010.
- [3] S. Ekarong, "Synergistic effects of alcohol-based renewable fuels: fuel properties and emissions," PhD thesis, University of Birmingham, 2013.
- [4] S.G. Michael, L. M. Robert, L. A. Teresa, and M. H. Andrew, "Effect of biodiesel composition on NO<sub>x</sub> and pm emissions from a DDC series 60 engine," *Tech. Rep.*, National Renewable Energy Laboratory, 1999.
- [5] L. Magin, A. Octavio, and R. Jose, "Effect of biodiesel fuels on diesel engine emissions," *Progress in Energy and Combustion Science*, vol. 34, pp. 198–223, 2008.
- [6] S. Dooley, F. L. Dryer, B. Yang, J. Wang, T. A. Cool, T. Kasper, and N. Hansen, "An experimental and kinetic modelling study of methyl formate low-pressure flames," *Combustion and Flame*, vol. 158, pp. 732–741, 2011.
- [7] S. Dooley, M. P. Burke, M. Chaos, Y. Stein, F. L. Dryer, V. P. Zhukov, O. Finch, J. M. Simmie, and H. J. Curran, "Methyl formate oxidation: speciation data, laminar burning velocities, ignition delay times, and a validated chemical kinetic model," *International Journal of Chemical Kinetics*, vol. 42, pp. 527–549, 2010.
- [8] J. S. Francisco, "Mechanistic study of gas-phase decomposition of methyl formate," *Journal of the American Chemical Society*, vol. 125, pp. 10475–10480, 2003.
- [9] W. K. Metcalfe, J. M. Simmie, and H. J. Curran, "Ab initio chemical kinetics of methyl formate decomposition: The simplest model biodiesel," *Journal of Physics and Chemistry*, vol. 114, pp. 5478–5484, 2010.
- [10] T. B. Hunter, B. H. Wang, T. A. Litzinger, and M. Frenklach, "The oxidation of methane at elevated pressures: Experiments and modeling," *Combustion and Flame*, vol. 97, pp. 201–224, 1994.
- [11] E. L. Petersen, D. F. Davidson, and R. K. Hanson, "Kinetics modeling of shock-induced ignition in low-dilution CH<sub>4</sub>/O<sub>2</sub> mixtures at high pressures and intermediate temperatures," *Combustion and Flame*, vol. 117, pp. 272–290, 1999.
- [12] S. Sibendu and K. A. Suresh, "A numerical investigation of methane air partially premixed flames at elevated pressures," *Combustion Science and Technology*, vol. 179, no. 6, pp. 1085–1112, 2007.
- [13] H. J. Curran, "Detailed chemical kinetic modelling: Is there life after GRIMECH 3.0," *Fuel Chem.*, vol. 49, no. 1, pp. 263–264, 2004.
- [14] D. D. Thomsen, F. F. Kuligowski, and N. M. Laurendeau, "Modeling of NO formation in premixed, high-pressure methane flames," *Combustion and Flame*, vol. 119, pp. 307–318, 1999.
- [15] G. Rozenchan, D. L. Zhu, C. K. Law, and S. D. Tse, "Outward propagation, burning velocities, and chemical effects of methane

- flames up to 60 atm,” *Proc. Combust. Inst.*, vol. 29, pp. 1461–1469, 2002.
- [16] T. J. Held and F. L. Dryer, “A comprehensive mechanism for oxidation of methanol,” *Chemical Kinetics*, vol. 30, pp. 805–830, 1998.
- [17] C. Sheng, J. W. Bozzelli, and I. Wen-chiun, “Development of a pressure dependent reaction model for methane/methanol mixtures under pyrolytic and oxidative conditions and comparison with experiment,” *Fuel Chemistry Division-New Jersey Institute of Technology, Newark*, vol. 47, no. 1, pp. 98–102, 2002.
- [18] S. M. DeCorso and J. S. Clark, “Stationary gas turbine alternative fuels,” *ASTM International*, 1983.
- [19] P. N. Kioni, J. K. Tanui, and A. Gitahi, “Numerical simulations of nitric oxide (NO) formation in methane, methanol and methyl formate in different flow configurations,” *Journal of Clean Energy Technologies*, vol. 1, pp. 151–156, 2013.
- [20] P. V. Rao, “Effect of properties of karanja methyl ester on combustion and NO<sub>x</sub> emissions of a diesel engine,” *Journal of Petroleum Technology and Alternative Fuels*, vol. 2, pp. 63–75, 2011.
- [21] K. Gerhard, C. A. Sharp, and T. W. Ryan, “Exhaust emissions of biodiesel, petrodiesel, neat methyl esters, and alkanes in a new technology engine,” *Energy and Fuel*, vol. 20, pp. 403–408, 2006.
- [22] S. R. Turns, *An Introduction to Combustion*, McGraw-Hill-Boston, 2000.
- [23] F. A. Williams, *The Fundamental Theory of Chemically Reacting Flow Systems*, the Benjamin/Cummings Publishing Company, Inc., 1985.
- [24] B. Rogg, “Adaptive methods in computational fluid dynamics of chemically reacting flows,” *Numerical Methods in Engineering*, vol. 90, pp. 659–670, 1991.
- [25] COSILAB Version 3. (2009). Rotexo-Cosilab GmbH & Co. KG, Bad Zwischenahn, Germany. [Online]. Available: [www.rotexo.com](http://www.rotexo.com)
- [26] G. P. Smith, D. M. Golden, M. Frenklach, N. W. Moriarty, B. Eiteneer, M. Goldenberg, C. T. Bowman, R. K. Hanson, S. Song, W. C. Gardiner Jr., and Z. Lissianski. Gri 3.0 mechanism. [Online]. Available: <http://www.me.berkeley.edu/gri-mech>
- [27] G. Wang, B. Zheng, Z. Huang, N. Zhang, Y. Zhang, and E. Hu, “Performance and emissions of a turbocharged, high pressure common rail diesel engine opera blendsting on biodiesel,” *Automotive Engineering*, vol. 225, pp. 127–148, 2010.
- [28] C. Sze, J. Whinihan, B. Olson, C. Schenk, and R. Sobotowski, “Impact of cycle test and biodiesel concentration on emissions,” *SAE Technical Paper*, vol. 4040, pp. 1–20, 2007.



**J. M. Ngugi** was born in Muranga, Kenya in 1986. He graduated with a MSc. degree in mechanical engineering (advanced thermo fluids) from Jomo Kenyatta University of Agriculture and Technology (JKUAT), Nairobi, in 2015. He obtained his BSc. (Hons) in mechanical engineering from the same university in 2011. He joined the Department of Mechanical Engineering of Dedan Kimathi University of Technology as a teaching assistant in August 2011.

Currently, he is an assistant lecturer and a PhD student. His main research interests are experimental and numerical studies of reactive flows with applications in flames and internal combustion engines. Mr. Ngugi is a graduate member of both the Engineers Board of Kenya (EBK) and the Institution of Engineers of Kenya (IEK).